Available online at www.sciencedirect.com

ScienceDirect

Physics Procedia 69 (2015) 314 – 319

Physics Procedia

10 World Conference on Neutron Radiography 5-10 October 2014

Laue Diffraction Using Scintillator Detectors

Gail N. Iles[a,*], Steven Peetermans[b], Susan Schorr[a,c], Eberhard Lehmann[b]

[a]*Department of Crystallography, Helmholtz-Zentrum Berlin, Hahn-Meitner Platz 1, 14109 Berlin, Germany*
[b]*Laboratory for neutron scattering and imaging, Paul Scherrer Institute, 5232 Villigen, Switzerland*
[c]*FreieUniversität Berlin, Institute of Geological Sciences, Malteserstr. 74-100, 12449 Berlin, Germany*

Abstract

The Fast Acquisition Laue Camera for Neutrons (FALCON) is a thermal neutron Laue diffractometer at HZB in Berlin. The instrument comprises two scintillator plate detectors coupled to four iCCD cameras each. One detector is placed in the backscattering position, enabling neutrons to pass through the centre of the detector box. The second detector is free to be placed either in the direct transmission position, or rotated to positions around the sample. The image-intensified CCDs, supplied by Photonic Science Ltd as components of the detector units, are capable of obtaining 20-bit digitization Laue images in under ten seconds. Whilst our instrument will be used as a diffractometer primarily for crystal structure determination, the configuration of the detectors is similar to ICON at PSI in Switzerland, especially in their 'double detector set-up'. In 2015 FALCON enters the commissioning phase whereby one of our activities will be to calibrate the detector units using CONRAD, the cold neutron imaging instrument of HZB. CONRAD will be used to characterise those factors which affect the total efficiency of the detectors i.e. cameras, lenses, CCD chips and the scintillators themselves e.g. homogeneity of the scintillator plate thickness.

Selection and peer-review under responsibility of Paul Scherrer Institut

Keywords: Neutron scattering; Laue diffraction; scintillator detectors; FALCON; neutron imaging

1. Introduction

The technique of Laue diffraction has been in practise for over 100 years, yet developments in instrumentation continue today. The ILL in Grenoble, France utilizes a number of Laue diffractometers, the original instruments

* Corresponding author. Current address: ANSTO, Lucas Heights, 2234 NSW, Australia; Tel.: +61 2 9717 9657; fax: +61 2 9717.
E-mail address: gail.iles@ansto.gov.au

Selection and peer-review under responsibility of Paul Scherrer Institut
doi:10.1016/j.phpro.2015.07.044

using image-plate detectors (Wilkinson 2002, Blakely 2010). More modern neutron Laue instruments use the more cost-effective scintillator detectors, at the expense of resolution (Ouladdiaf 2006, 2011). Neutron scintillators are also popular for detectors in the field of neutron imaging.

We present here the commissioning activities proposed for FALCON, a newly-built diffractometer at HZB (Germany), and data recently collected at ICON, the imaging instrument at PSI (Switzerland). The 'double-detector set-up' of ICON using scintillator detectors is capable of simultaneously measuring at diffraction angles and in the imaging transmission position. A full definition of this configuration is described by Peetermans and Lehmann (2013). The data presented is from a Cu_2ZnSnS_4 single-crystal round-robin sample that will also be used during the commissioning of FALCON. Additional investigations of the FALCON detector boxes will take place on the CONRAD instrument beam position, also at HZB.

2. FALCON: Laue Diffractometer

The Fast Acquisition Laue Camera for Neutrons (FALCON) was completed in 2014 as reported by Iles and Schorr (2012- 2015). The instrument comprises two scintillator detectors; one permanently in the backscattering position, the second free to rotate about a sample positioned between the two detectors. A diagram of the layout is shown in figure 1.

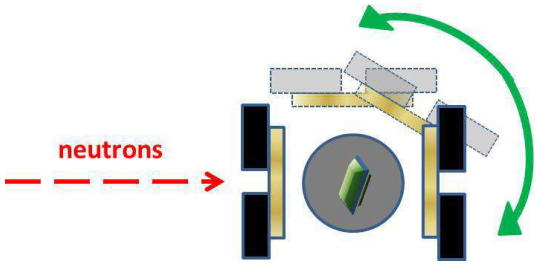

Fig. 1. FALCON schematic layout. The neutrons pass through the backscattering scintillator which is fixed in place, whilst the second detector is free to be rotated about the sample.

The flux at the instrument should be of the order of 10^8 n cm^{-2} s^{-1} with a wavelength distribution consistent with a thermal neutron profile i.e. $0 < \lambda < 6$Å, peaking around 1.4Å Each 40cm^2 detector is coupled to four iCCDs and the incident beam divergence is ~1°. Sample – detector distances can be varied depending upon the nature of the experiment. For simple orienting, the sample can be brought as close as 1cm to the backscattering detector. Alternatively, if it is required to use large sample environment e.g, 5T magnet, the sample – detector distance would be ~ 50cm.

2.1 Scientific research areas

A neutron Laue diffractometer is a versatile instrument allowing a range of cutting-edge science to be performed. Of particular interest for the intensive research programme in renewable energies implemented at HZB is to fully investigate the nature of the site defects in Cu_2ZnSnS/Se_4 (CZTS) materials. Schorr (2011) showed that the efficiency of such materials as solar cell absorber materials could be improved by varying the ratio of S to Se in the quaternary compound. However, anti-site defects between the Cu and Zn alter the band gap in the semiconductors and the mechanism for this is not well understood. FALCON can provide structural information on these compounds that cannot be obtained through powder diffraction measurements.

FALCON is fully compatible with a full range of sample environments and therefore the instrument is of use for studies in low temperature magnetism, for example. Toft-Petersen et al (2012) observed an increased intensity of the Lorentz broadened elastic scattering at magnetic Bragg peaks above T_N as compared to zero field and 10T,

without an increase in peak width in $LiMnPO_4$. Whilst this system is well understood, behaviour of a similar compound - LiCoPO4 - remains a mystery with no knowledge of the phase boundaries at low temperature. FALCON can be equipped with the VM-3 5T magnet to obtain large scans of reciprocal space on this sample to better map the unknown regions of the phase diagram.

2.2 Technical features

An important feature of this unique instrument is the ability to take a single measurement in seconds, rather than the typical minutes, or hours of a standard neutron scattering measurement. The image-intensifiers coupled to the CCDs amplify the signal generated by the conversion of neutrons into photons by the scintillator allowing samples which are weak scatterers to be imaged successfully. With digitization set to 16-bit mode, i.e. differentiating 216 grey levels, FALCON can take a single measurement in 0.5s. If the sample is particularly small, or scatters weakly, the option to increase the grey levels to 20-bit digitization is offered, requiring a measurement time of 8s. Such fast exposures open the field of science to in situ kinetics studies such as how hydrates form.

Finally, FALCON has a versatile beam selection function whereby the beam size can be varied to suit the sample being measured. The exit port from the backscattering detector is 20mm in diameter, however, variable size diameters can be added offering a beam size from just 1mm diameter up to 20mm in 1mm steps. Such an intense and precise beam is ideal for studying small samples or samples with a restricted view such as a Paris-Edinburgh cell, Besson et al (1992).

3. ICON

ICON is the cold neutron imaging facility at the neutron spallation source SINQ, Kaestner (2011). The beamline offers specialized instrumentation for imaging with cold neutrons. The standard configuration allows radiography and tomography with a field of view from 30mm to 250mm. An aperture wheel makes it possible to change beam intensity and collimation ratio. In addition to the standard setup it is possible to add beam modifying components for energy selective imaging and grating interferometry.

We obtained beamtime on ICON to measure the single-crystal, Cu_2ZnSnS_4, a compound of significant interest in the search for cost-effective solar cell absorber materials (Schorr 2011).

3.1 CZTS measured on ICON

We operated ICON in the double-detector setup with an aperture of 40mm. Tomography measurements were made in 375 steps from 0-360°. The specific details for each detector are listed in Table 1 where the Micro setup refers to the imaging detector at 0° to the beam, and the Midi setup refers to the diffraction detector perpendicular to the neutron beam.

Table 1. Detector configuration on ICON

	Micro set-up	**Midi set-up**
Angle	0°	180°
Pixelsize	13.5µm	55µm
Exposure time	130s	150s
Scintillator	20µm Gadox	100µm Li-6
Field-of-view	27.6x27.6mm^2	119.5x141.6mm^2

The initial reconstructed transmission tomography image is shown in figure 2a. This shows the distribution of material (crystal, porosities, plasticine) throughout the sample in a standard filtered projection. It is interesting to note that a large pore is visible within the crystal. This may be due to the manufacture process of the crystal.

For the diffraction measurements, after determining the background level and noise full-width half-maximum, we could find the segmentation parameters. Using this method we determined the location of a Bragg reflection obtaining information such as pixel position of centre of mass and the intensity of the reflection. For comparison, when we look at the diffraction spots from the detector placed at 180° to the beam, the Bragg reflections actually take the shape of the crystal itself, as can be seen in figure 2b. The highlighted Bragg reflection is the most easily seen from this image, however, it is possible to see other reflections around the central area. (The square in the centre of figure 2b is the direct beam and therefore not imaged.)

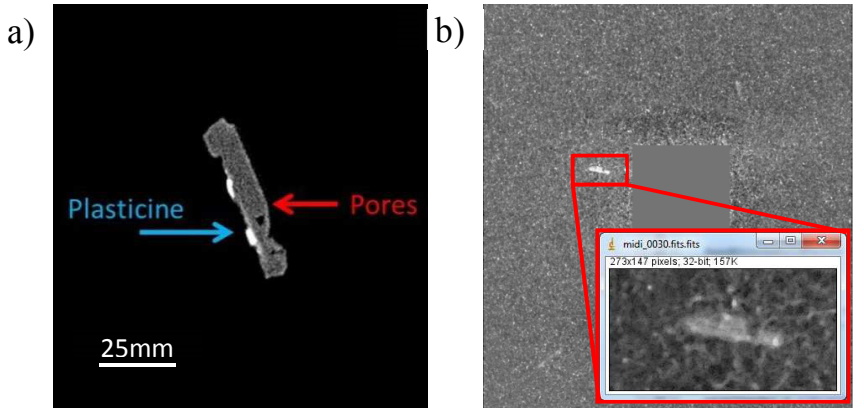

Fig. 2. Images of a Cu_2ZnSnS_4 single-crystal a) in reconstructed transmission tomography and b) as a diffraction projection (sample-detector distance ~10cm)

For the diffraction spots to have taken on the shape of the original crystal firstly indicates that the sample is a very pure single-crystal, however, as elliptical spots are generated by extinction from overly large samples, it will be difficult to obtain any structural information from these images.

Continuing with the reconstruction of the tomography images, the fully rendered images are shown in figure 3. Here we show the transmission render in figure 3a, the diffraction contrast tomography render in figure 3b and the combination of these in figure 3c.

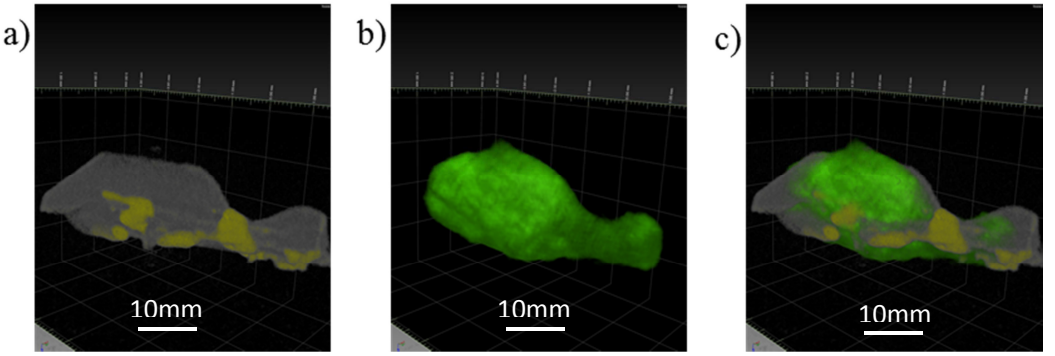

Fig. 3. Rendering of Cu_2ZnSnS_4 single-crystal in a) transmission b) diffraction contrast tomography c) transmission + diffraction contrast combined (Yellow patches are residual plasticine from mounting)

The diffraction contrast tomography in figure 3b is an algebraic reconstruction using the Simultaneous iterative reconstruction technique (SIRT) in 3-D and the ASTRA reconstruction package for Matlab, a method described by Palenstijn et al (2011). In order to produce the image in figure 3b, 10 iterations were performed.

3.2 Diffraction data analysis

In the images in figure 3 it is easy to see the physical shape of the crystal. The diffraction image clearly does not cover the entire volume of the crystal implying a different structure, or even phase, at the boundaries. Whilst ICON has been used previously by the authors to demonstrate the use in identifying different grains in polycrystalline samples, Peetermans (2014), the diffraction data will be difficult to analyse using standard Laue diffraction software. A typical Laue diffraction image contains many Bragg reflections which ideally are near-circular. Analysis software for such data is specifically designed to reject data points that are overly elliptical in shape and therefore diffraction data from ICON is not yet suitable for producing diffraction datasets. However, the grains would not be visible in a typical Laue diffraction image, for example as will be obtained with FALCON, and therefore, this data is useful and complementary. That our CZTS crystal shows differing areas of diffraction throughout the crystal is very interesting and such information will contribute to understanding the growth mechanics of the crystal.

4. CONRAD

The **Co**ld **N**eutron **Rad**iography (CONRAD) instrument at HZB is described by Kardjilov et al (2011). CONRAD was designed with two measuring positions: high-flux and high-resolution. In high flux mode the sample is located directly at the end of the neutron guide, where image resolution is limited due to the beam divergence. This measuring position allows unique experiments in the field of real-time imaging and high-speed tomography with exposure times ranging from 10 ms to 500 ms. The achieved resolution varies from 300μm to 500μm dependent on the distance between the sample and the detector. The second measuring position i.e. high resolution mode, uses a pin-hole geometry followed by more than 5m of flight tube in order to gain a high collimation ratio and image resolution. In this configuration, a resolution of 100μm is achieved, with exposure times of 1-25s.

4.1 Commissioning of the FALCON detector boxes

Considering the two instrument options available at CONRAD i.e. high flux or high resolution, there is 5m of available space on the beamline directly after the end of the neutron guide. Even with the pinhole collimator in place, ~1m^3 of space still remains at the sample position. We propose to take one of the FALCON detector boxes ~450x600x400mm in size i.e. containing 400x400mm scintillator plate coupled to four iCCDs and place it in the neutron beam of CONRAD. This will allow us to characterize those factors that affect the efficiency of such a system. When imaging, or performing Laue diffraction, it is essential to know very well the thickness of the scintillator plate. The FALCON scintillators are 250μm in thickness, a feature which dictates the efficiency of the plate i.e. the ratio of neutrons converted into photons. This efficiency also depends on the nature of the neutron beam i.e. ~45% efficiency for thermal neutrons (FALCON position) and ~55% efficiency for cold neutrons (CONRAD position). For FALCON operating in a thermal neutron beam profile, this efficiency will be ~25%, with a cold neutron beam profile, this will raise to ~40%. However, if the plate is not of a uniform thickness, this will affect the efficiency of the plate in these areas. Tolerances of the plate thickness could be as large as +/- 50μm. Such variances would affect the intensity of any Bragg reflections located in ‘thicker’ or ‘thinner’ areas.

4.2 FALCON flat-field correction

One of the most important corrections to be made on FALCON is the flat-field correction. Flat fielding refers to the process of compensating for different gains and dark currents in a detector. After this correction, ideally, artifacts caused by variations in the pixel-to-pixel sensitivity of the detector and/or by distortions in the optical path are removed from the 2-D images. Artifacts could be generated by excess gamma radiation, or ambient light

leaking into the detector boxes, for example. Once a detector has been appropriately flat-fielded, a uniform signal will create a uniform output (hence flat-field). This then means any further signal is due to the Bragg reflections, for example, and not a systematic error. Distortions in the optical path can come from the cameras, the lenses and the iCCD chips. The measurements on CONRAD can assist in the characterization of all factors affecting the quality of images obtained by FALCON in the future.

5. Conclusion

We have described the similarities between Laue diffractometers with scintillator detectors and neutron imaging instruments. Diffraction data can be obtained from an imaging instrument to provide information about grain size in polycrystalline samples or phase boundaries in single-crystals. We presented data from ICON on a single-crystal sample of Cu_2ZnSnS_4 which showed that the sample contained a large pore, possibly forming during the growth process.

We also highlighted some of the future work involved in calibrating the FALCON detectors by using the CONRAD beamline at the HZB. Establishing the flat-field of FALCON will be critical to producing reliable datasets in the future.

Acknowledgements

We gratefully acknowledge funding from the Helmholtz Association for the construction of FALCON.

References

Besson J.M., Nelmes R.J., Hamel G., Loveday J.S., Weill G., Hull S., 1992. Neutron Powder Diffraction above 10GPa. *Physica B* **180–181** 907.

Blakeley M.P., Teixeira S.C.M., Petit-Haertlein I., Hazemann I., Mitschler A., Härtlein M., Howard E. Podjarny A.D., 2010. Neutron macromolecular crystallography with LADI-III. *Acta Cryst. D* **66** 1198-1205

Iles G.N., Schorr S., 2012. The New Neutron Laue Diffractometer at HZB. *Acta Cryst.* **A68**, s134.

Iles G.N., Schorr S., 2014. Commissioning the Neutron Laue Diffractometer in Berlin. *Acta Cryst.* **A70**, C1742.

Iles G.N., Schorr S., 2014. The HZB neutron Laue diffractometer – from E11 to FALCON. *Neutron News* **25,** 2.

Iles G.N., Schorr S., 2015. The new single-crystal neutron Laue diffractometer in Berlin. *Journal of Neutron Research.*

Kaestner A.P., Hartmann S., Kühneb G., Freib G., Grünzweiga C., Josica L., Schmida F., Lehmann E.H.., 2011. The ICON beamline – A facility for cold neutron imaging at SINQ. *Nucl. Instrum. Meth. A* **659**, Issue 1, 387–393.

Kardjilov N., Hilger A., Manke I., Strobl M., Dawson M., Williams S., Banhart J., 2011. Neutron tomography instrument CONRAD at HZB. *Nucl. Instrum. Meth. A* **651** 47-52.

Ouladdiaf B., Archer J., McIntyre G.J., Hewat A.W., Brau D. York S., 2006. OrientExpress: A new system for Laue neutron diffraction. *Physica B* **385–386** 1052–1054

Ouladdiaf B., Archer J., Allibon J.R., Decarpenterie P., Lemée-Cailleau M-H, Rodríguez-Carvajal J., Hewat A.W., York S., Brau D. McIntyre G.J. 2011. CYCLOPS – a reciprocal-space explorer based on CCD neutron detectors. *J. Appl. Cryst.* **44** 392-397

Palenstijn W.J., Batenburg K.J., Sijbers J., 2011. Performance improvements for iterative electron tomography reconstruction using graphics processing units (GPUs). *J. Struct. Biol.* **176**, 250-253.

Peetermans S., Lehmann E.H., 2013. Simultaneous neutron transmission and diffraction contrast tomography as a non-destructive 3D method for bulk single crystal quality investigations. *J. Appl. Phys.* **114**, 124905.

Peetermans S., King A., Ludwig W., Reischig P., Lehmann E., 2014. Cold neutron diffraction contrast tomography of polycrystalline material. *Analyst* **139**(**22**):5765-71.

Schorr S., 2011. The crystal structure of kesterite type compounds: a neutron and X-ray diffraction study. *Sol En Mat Sol Cells* **95** 1482-1488.

Toft-Petersen R., Andersen N.H., Li H., Li J., Tian W., Bud'ko S.L., Jensen T.B.S., Niedermayer C., Laver M., Zaharko O., Lynn J.W., Vaknin D., 2012. Magnetic phase diagram of magnetoelectric $LiMnPO_4$. *Phys. Rev. B* **85**, 224415.

Wilkinson C., Cowan J.A., Myles D.A.A., Cipriani F. McIntyre G.J., 2002. VIVALDI - A Thermal-Neutron Laue Diffractometer for Physics, Chemistry and Materials Science. *Neutron News* **13** 37-4